

Modeling and Dynamic Analysis of hybrid synchronous machine

Eugene Okenna Agbachi
Department of Electrical and
Electronics Engineering
Federal University of Technology
Minna, Nigeria
euokenna@futminna.edu.ng

Linus Uchekukwu Anih
Department of Electrical Engineering
University of Nigeria
Nsukka, Nigeria
linus.anih@unn.edu.ng

Emeka Simon Obe
Department of Electrical Engineering
University of Nigeria
Nsukka, Nigeria
simon.obe@unn.edu.ng

Abstract— The modeling and dynamic analysis of hybrid synchronous machine is presented. This modelled machine, comprises a salient-pole and round rotor machine components with each having two sets of identical windings referred to as main and auxiliary windings. The q-axis reactance could be varied by varying the capacitor on the auxiliary winding of the machine. In this case, the reactance ratio (x_D/x_Q) on which the reluctance torque depends can increase theoretically to infinity.

It is shown that unlike the conventional synchronous machine which has small reluctance torque, the hybrid machine has the capability of producing reluctance torque that is twice the excitation torque. The modelled machine under ramp loading demonstrated higher loading capability

Keywords—Synchronous machine, hybrid, reluctance torque, reactance ratio.

I. INTRODUCTION

The reluctance torque component of a typical synchronous machine is negligible when compared with the excitation component. This is as a result of low saliency ratio (x_d/x_q) upon which the reluctance torque depends [1]. The attempts to enhance the (x_d/x_q) ratio has been to reduce the x_q ; which has an attendant reduction of x_d as well. Effective enhancement of the saliency ratio will have a positive effect on the output power, torque and the power factor. Some studies that have been carried out to achieve high saliency ratio include redesign of the rotor geometry [2]–[5], double stator winding and capacitor injection [6].

This research intends to make the reluctance torque of a synchronous machine high by adapting the approach in [1] to a salient pole and round rotor synchronous machine in which case, the round rotor half will contribute to the output power.

II. FUNDAMENTAL CONCEPT OF HYBRID SYNCHRONOUS MACHINE

The hybrid synchronous machine comprises a salient-pole and a round-rotor elemental synchronous machines that are mechanically coupled and each machine having two sets of identical stator winding. One set of the windings is transposed across the machine halves while the other is in series. The windings are referred to as the main and auxiliary windings and, while the main winding is connected to the mains, the auxiliary winding is connected to a capacitor bank as in fig. 1 The synchronous reactance x_s of the round rotor half is made equal to the d-axis reactance x_d of the of the salient pole half

such that when the salient pole half operates on the d-axis, the overall d-axis reactance will be $x_D = x_d + x_d = 2x_d$. Also, when the salient pole half operates on the q-axis, the overall q-axis reactance will be $x_Q = x_d + x_q$.

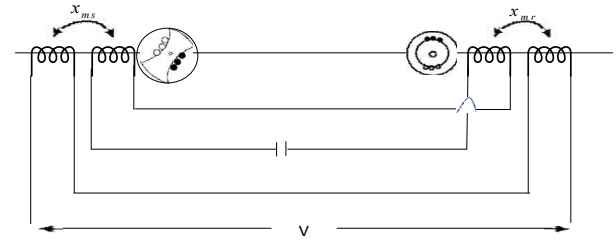


Figure 1: Schematic diagram of the hybrid synchronous machine

It is shown that the overall q-axis reactance depends on the value of the capacitor on the auxiliary winding, and can be made zero, thereby making the reactance ratio (x_D/x_Q) infinity [7], [8].

III. MATHEMATICAL MODEL OF THE HYBRID SYNCHRONOUS MACHINE

The modelling of this machine, is based on the approached that are available in a classical text for the modeling of a typical synchronous machine [9], [10]

The stator and rotor windings are sinusoidally distributed.

A. Stator Voltage Equation

In this modelling, the main winding will be represented by abc while the auxiliary winding will be represented as xyz .

B. Main Winding ((abc))

The voltage equations are

$$V_{abc} = R_s I_{abc} + P \lambda_{abc} \quad (1)$$

where,

$$\begin{cases} V_{abc} = [V_{as} \ V_{bs} \ V_{cs}]^T \\ I_{abc} = [I_{as} \ I_{bs} \ I_{cs}]^T \\ \lambda_{abc} = [\lambda_{as} \ \lambda_{bs} \ \lambda_{cs}]^T \\ R_s = \text{diag}[R_s \ R_s \ R_s] \end{cases} \quad (2)$$

The flux linkage equation is given as

$$\lambda_{abc} = L_{abc} I_{abc} + L_{abcxyz} I_{xyz} + L_{abcqdr} I_{qdr} \quad (3)$$

where;

$L_{abc} I_{abc}$ = flux linkage due to abc stator winding current

$L_{abcxyz} I_{xyz}$ = flux linkage due to the current in xyz stator winding

$L_{abcqdr} I_{qdr}$ = flux linkage due to the rotor winding current

The subscript abc is for the main windings while xyz is for the auxiliary winding

C. Inductance Matrix

L_{abcs} = main winding inductance matrix.

The main winding inductance is the summation of the inductances of the salient pole and the round rotor half of the machine. This is given in the expression below;

$$L_{abc} = L_{SS}(\text{salient pole machine}) + L_{RR}(\text{Round rotor machine}) \quad (4)$$

$$L_{abc} = L_{SS} + L_{RR} = \begin{bmatrix} 2L_s + L_1 - L_m \cos 2\theta_r & -L_2 - L_m \cos 2(\theta_r - \frac{\pi}{3}) & -L_2 - L_m \cos 2(\theta_r + \frac{\pi}{3}) \\ -L_2 - L_m \cos 2(\theta_r - \frac{\pi}{3}) & 2L_s + L_1 - L_m \cos 2(\theta_r - \frac{2\pi}{3}) & -L_2 - L_m \cos 2(\theta_r + \pi) \\ -L_2 - L_m \cos 2(\theta_r + \frac{\pi}{3}) & -L_2 - L_m \cos 2(\theta_r + \pi) & 2L_s + L_1 - L_m \cos 2(\theta_r + \frac{2\pi}{3}) \end{bmatrix} \quad (5)$$

where;

$$L_1 = L_{md} + \frac{1}{3}L_{mq} \text{ and } L_2 = \frac{1}{2}L_{md} + \frac{1}{6}L_{mq}$$

L_{abcxyz} = mutual inductance between the main and auxiliary winding

On the assumption that the main and auxiliary windings are identical and are mutually coupled and occupy the same slot position, it implies that the mutual inductance between the two sets are equal, and each of them is equal to self-inductance minus the leakage inductance[1].

Therefore, if, L_{MS} is the mutual inductance of the salient pole side; then, $L_{MS} = L_{SS} - L_l$. Also, for the round rotor,

$$L_{MR} = L_{RR} - L_l$$

Since the auxiliary winding of the machine is transposed, the direction of current flow will aid the main current in one half of the machine and in opposition to the main current in the other half.

$$\begin{aligned} \therefore L_{abcxyz} &= L_{RR} - L_l - (L_{SS} - L_l) \\ &= L_{RR} - L_{SS} \\ &= \begin{bmatrix} L_3 + L_m \cos 2\theta_r & L_4 + L_m \cos 2(\theta_r - \frac{\pi}{3}) & L_4 + L_m \cos 2(\theta_r + \frac{\pi}{3}) \\ L_4 + L_m \cos 2(\theta_r - \frac{\pi}{3}) & L_3 + L_m \cos 2(\theta_r - \frac{2\pi}{3}) & L_4 + L_m \cos 2(\theta_r + \pi) \\ L_4 + L_m \cos 2(\theta_r + \frac{\pi}{3}) & L_4 + L_m \cos 2(\theta_r + \pi) & L_3 + L_m \cos 2(\theta_r - \frac{2\pi}{3}) \end{bmatrix} \end{aligned} \quad (6)$$

$$\text{where } L_3 = \frac{L_{md} - L_{mq}}{3} \text{ and } L_4 = \frac{L_{mq} - L_{md}}{6}$$

L_{abcqdr} = Mutual inductance between the main winding and the rotor winding

This is the sum of the mutual inductances of the salient pole half and the mutual inductance of the round rotor half.

$$L_{abcqdr} = [L_{abcqdr}]_{RR} + [L_{abcqdr}]_{SS} = \begin{bmatrix} (L_{md} + L_{mq}) \cos \theta_r & 2L_{md} \sin \theta_r & 2L_{md} \sin \theta_r \\ (L_{md} + L_{mq}) \cos(\theta_r - \frac{2\pi}{3}) & 2L_{md} \sin(\theta_r - \frac{2\pi}{3}) & 2L_{md} \sin(\theta_r - \frac{2\pi}{3}) \\ (L_{md} + L_{mq}) \cos(\theta_r + \frac{2\pi}{3}) & 2L_{md} \sin(\theta_r + \frac{2\pi}{3}) & 2L_{md} \sin(\theta_r + \frac{2\pi}{3}) \end{bmatrix} \quad (7)$$

The Auxiliary Winding (xyz)

The auxiliary winding is connected across a balanced capacitor bank and transposed across the two machine halves.

The voltage equation for the winding is as (8)

$$V_{xyz} = R_{xyz} I_{xyz} + p\lambda_{xyz} + V_{c_{xyz}} \quad (8)$$

where

$$\begin{cases} V_{xyz_s} = [V_{xs} \ V_{ys} \ V_{zs}]^T \\ I_{xyz_s} = [I_{xs} \ I_{ys} \ I_{zs}]^T \\ \lambda_{xyz_s} = [\lambda_{xs} \ \lambda_{ys} \ \lambda_{zs}]^T \\ V_{c_{xyz_s}} = [V_{c_{xs}} \ V_{c_{ys}} \ V_{c_{zs}}]^T \\ R_{xyz_s} = \text{diag}[R_s \ R_s \ R_s] \end{cases} \quad (9)$$

The current I_{xyz_s} is expressed in terms of capacitor voltage,

since the current in the winding is as result of the capacitor

$$\therefore I_{xyz_s} = c \frac{d}{dt} V_{c_{xyz_s}} \quad (10)$$

The flux linkage for the auxiliary winding is expressed as;

$$\lambda_{xyz_s} = L_{xyzabc} I_{abc} + L_{xyz} I_{xyz} + L_{xyzqdr} I_{qdr} \quad (11)$$

where

$L_{xyzabc} I_{abc}$ = flux linkage due to abc stator winding current

$L_{xyz} I_{xyz}$ = flux linkage due to the current in xyz stator winding

$L_{xyzqdr} I_{qdr}$ = flux linkage due to the rotor winding current

Since the main and the auxiliary windings are identical and occupy the same slot position, then

$$\begin{cases} L_{xyzabc} = (L_{abcxyz})^T \\ L_{xyz} = L_{abc} \end{cases} \quad (12)$$

Due to the transposition of the auxiliary winding between the two-machine halves, the mutual inductance between the auxiliary winding and the rotor winding will be the algebraic sum of the mutual inductances of the two machine halves.

$$L_{xyzqdr} = [L_{xyzqdr}]_{RR} - [L_{xyzqdr}]_{SS} = \begin{bmatrix} (L_{md} - L_{mq}) \cos \theta_r & 0 & 0 \\ (L_{md} - L_{mq}) \cos(\theta_r - \frac{2\pi}{3}) & 0 & 0 \\ (L_{md} - L_{mq}) \cos(\theta_r + \frac{2\pi}{3}) & 0 & 0 \end{bmatrix} \quad (13)$$

Rotor Voltage Equations

The rotor circuit is equipped with field and two caged windings. The field winding is on the d-axis while caged winding is on both the d-axis and q-axis.

The voltage equation is as shown;

$$V_{qdr} = R_{qdr} I_{qdr} + p\lambda_{qdr} \quad (14)$$

where

$$\begin{cases} V_{qdr} = [V_{qr} \ V_{dr} \ V_{df}]^T \\ I_{qdr} = [I_{qr} \ I_{dr} \ I_{df}]^T \\ \lambda_{qdr} = [\lambda_{qr} \ \lambda_{dr} \ \lambda_{df}]^T \\ R_{qdr} = \text{diag}[R_{qr} \ R_{dr} \ R_{df}] \end{cases} \quad (15)$$

The flux linkage equations for the rotor winding are given by

$$\lambda_{qdr} = L_{qdrabc} I_{abc} + L_{qdrxyz} I_{xyz} + L_{qdr} I_{qdr} \quad (16)$$

where

L_{qdrabc} = mutual inductance between the rotor and main windings of the stator

L_{qdrxyz} = mutual inductance between the rotor and auxiliary windings of the stator

L_{qdr} = Self-inductance of the rotor winding

Since the main and auxiliary windings of the stator are identical and occupy the same slot, then

$$L_{qdrabc} = [L_{abcqdr}]^T \quad (17)$$

$$L_{qdrxyz} = [L_{xyzqdr}]^T \quad (18)$$

$$L_{qdr} = [L_{qdr}]_{RR} + [L_{qdr}]_{SS} = \begin{bmatrix} L_{lq} + L_{mq} + L_{ld} + L_{md} & 0 & 0 \\ 0 & 2(L_{ld} + L_{md}) & 2L_{md} \\ 0 & 2L_{md} & 2(L_{lf} + L_{md}) \end{bmatrix} \quad (19)$$

The Hybrid Machine Voltage Equations

The voltage equations describing the hybrid machine are as shown;

$$\begin{cases} V_{abc} = R_{abc}I_{abc} + p\lambda_{abc} \\ V_{xyz} = R_{xyz}I_{xyz} + p\lambda_{xyz} + V_{cxyz} \\ V_{qdr} = R_{qdr}I_{qdr} + p\lambda_{qdr} \end{cases} \quad (20)$$

While the flux linkages are

$$\begin{cases} \lambda_{abc} = L_{abc}I_{abc} + L_{abcxyz}I_{xyz} + L_{abcqdr}I_{qdr} \\ \lambda_{xyz} = L_{xyzabc}I_{abc} + L_{xyz}I_{xyz} + L_{xyzqdr}I_{qdr} \\ \lambda_{qdr} = L_{qdrabc}I_{abc} + L_{qdrxyz}I_{xyz} + L_{qdr}I_{qdr} \end{cases} \quad (21)$$

Transformation to qdo

The inductance matrix of equations of (5), (6), (7) and (13) have some parts that are rotor dependent. This rotor dependence can be eliminated by transforming to the rotor reference frame using park's transformation equation as shown in equation(22).

$$T_{qdo}(\theta_r) = \frac{2}{3} \begin{bmatrix} \cos\theta_r & \cos(\theta_r - \frac{2\pi}{3}) & \cos(\theta_r + \frac{2\pi}{3}) \\ \sin\theta_r & \sin(\theta_r - \frac{2\pi}{3}) & \sin(\theta_r + \frac{2\pi}{3}) \\ \frac{1}{2} & \frac{1}{2} & \frac{1}{2} \end{bmatrix} \quad (22)$$

The transformed flux linkage equations are given equations (23) and (24)

$$\begin{bmatrix} \lambda_{Qs} \\ \lambda_{qs} \\ \lambda_{qcg} \end{bmatrix} = \begin{bmatrix} 2L_{ls} + L_{md} + L_{mq} & L_{md} - L_{mq} & L_{md} + L_{mq} \\ L_{md} - L_{mq} & 2L_{ls} + L_{md} + L_{mq} & L_{md} - L_{mq} \\ L_{md} + L_{mq} & L_{md} - L_{mq} & L_{ld} + L_{lq} + L_{md} + L_{mq} \end{bmatrix} \begin{bmatrix} I_{Qs} \\ I_{qs} \\ I_{qcg} \end{bmatrix} \quad (23)$$

$$\begin{bmatrix} \lambda_{Ds} \\ \lambda_{ds} \\ \lambda_{dcg} \\ \lambda_{df} \end{bmatrix} = \begin{bmatrix} 2(L_{ls} + L_{md}) & 0 & 2L_{md} & 2L_{md} \\ 0 & 2(L_{ls} + L_{md}) & 0 & 0 \\ 2L_{md} & 0 & 2(L_{ld} + L_{md}) & 2L_{md} \\ 2L_{md} & 0 & 2L_{md} & 2(L_{lf} + L_{md}) \end{bmatrix} \begin{bmatrix} I_{Ds} \\ I_{ds} \\ I_{dcg} \\ I_{df} \end{bmatrix} \quad (24)$$

The qdo Voltage equations

The voltage equations in machine variable is given as;

$$V_{abc} = 2R_s I_{abc} + P\lambda_{abc} \quad (25)$$

This machine variables can be transformed to qdo as shown by Ong[10]

$$V_{qdo} = T_{qdo} R_s T_{qdo}^{-1} I_{qdo} + T_{qdo} P T_{qdo}^{-1} \lambda_{qdo} \quad (26)$$

Simplifying this gives

$$V_{qdo} = 2R_s I_{qdo} + \omega_r \begin{bmatrix} 0 & 1 & 0 \\ -1 & 0 & 0 \\ 0 & 0 & 0 \end{bmatrix} \lambda_{qdo} + P\lambda_{qdo} \quad (27)$$

Now simplifying equation (27) and representing main winding components with capital letters while representing auxiliary winding components with small letters, gives

$$\begin{cases} V_{Qs} = 2r_s I_{Qs} + \omega_r \lambda_{Ds} + P\lambda_{Qs} \\ V_{Ds} = 2r_s I_{Ds} - \omega_r \lambda_{Qs} + P\lambda_{Ds} \\ V_{Os} = 2r_s I_{Os} + P\lambda_{Os} \\ V_{qs} = 2r_s I_{qs} + \omega_r \lambda_{ds} + P\lambda_{qs} + V_{cq} \\ V_{ds} = 2r_s I_{ds} - \omega_r \lambda_{qs} + P\lambda_{ds} + V_{cd} \\ V_{os} = 2r_s I_{os} + P\lambda_{os} + V_{co} \\ V_{qcg} = 2r_{cg} I_{qcg} + P\lambda_{qcg} = 0 \\ V_{dcg} = 2r_{cg} I_{dcg} + P\lambda_{dcg} = 0 \\ V_{df} = 2r_f I_f + P\lambda_f \end{cases} \quad (28)$$

D. The Equivalent Circuit of the Hybrid Machine Model

The dynamic equivalent circuit of the hybrid machine model is drawn based on equations (23), (24) and (28) and it is shown in figure 2

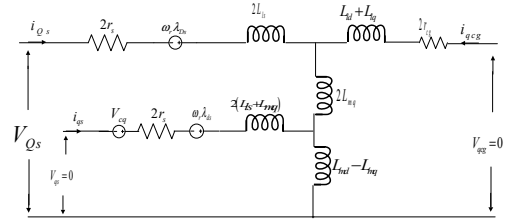


Figure 2a: Q-axis equivalent circuit of the hybrid synchronous machine

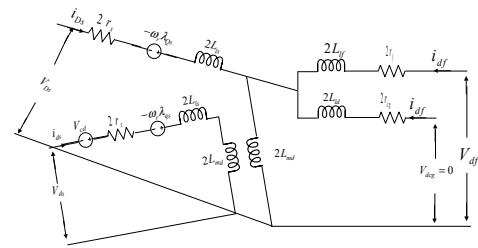


Figure 2b: D-axis Equivalent Circuit of the Hybrid Synchronous Machine

E. Capacitor Voltage Equation

The auxiliary winding of the machine is connected to a balanced capacitor.

For the three-phase capacitive circuit connected to the auxiliary winding,

$$i_{zxy} = \frac{d}{dt} q_{xyz} \quad (29)$$

Applying Park's transformation equations to (29) and simplifying gives

$$pV_{cq} = \frac{i_{qc}}{C} - \omega_r V_{cd} \quad (30)$$

$$pV_{cd} = \frac{i_{dc}}{C} + \omega_r V_{cq} \quad (31)$$

Since the auxiliary winding of this machine is short-circuited, the current in the winding will be the current as a result of the capacitor. Therefore $i_{qc} = I_{qs}$ and $i_{dc} = I_{ds}$ as in equation (30) and (31)

IV. THE ELECTROMAGNETIC TORQUE

The total input power to the machine in qdo variable is given as;

$$P_{qdo} = \frac{3}{2}(V_{Qs}I_{Qs} + V_{Ds}I_{Ds} + 2V_{Os}I_{Os} + V_{qs}I_{qs} + V_{ds}I_{ds} + 2V_{os}I_{os} + V_f I_f) \quad (32)$$

Substituting equation 34 into equation 38 gives

$$P_{in} = \frac{3}{2} \left\{ \underbrace{(r_s(I_{Ds}^2 + I_{Qs}^2 + I_{ds}^2 + I_{qs}^2) + r_f I_f^2)}_{\text{Power loss}} + \underbrace{\omega_r(\lambda_{Ds}I_{Qs} - \lambda_{Qs}I_{Ds}) + \omega_r(\lambda_{ds}I_{qs} - \lambda_{qs}I_{ds})}_{\text{Energy conversion}} + \underbrace{I_{Ds}P\lambda_{Ds} + I_{Qs}P\lambda_{Qs} + I_{ds}P\lambda_{ds} + I_{qs}P\lambda_{qs} + I_f P\lambda_f}_{\text{Energy stored}} + \underbrace{V_{cd}I_{ds} + V_{cq}I_{qs}}_{\text{Energy stored in capacitor}} \right\} \quad (33)$$

From equation (33), the second term is the part that indicates the electrical to mechanical energy conversion. Therefore, the electromagnetic power is given as

$$P_{em} = \frac{3}{2}[\omega_r(\lambda_{Ds}I_{Qs} - \lambda_{Qs}I_{Ds}) + \omega_r(\lambda_{ds}I_{qs} - \lambda_{qs}I_{ds})] \quad (34)$$

For a P-pole machine, $\omega_r = \left(\frac{P}{2}\right)\omega_{rm}$;

where ω_{rm} is the rotor speed in mechanical radians per second. The expression for the electromagnetic torque is written from (34) as

$$T_{em} = \frac{3P}{2} \{ (\lambda_{Ds}I_{Qs} - \lambda_{Qs}I_{Ds}) + (\lambda_{ds}I_{qs} - \lambda_{qs}I_{ds}) \} \quad (35)$$

Substituting (23) and (24) into (35), we have

$$T_{em} = \frac{3P}{2} \left\{ \underbrace{(L_{md} - L_{mq})i_{Ds}i_{Qs} + (L_{md} - L_{mq})i_{ds}i_{qs} + (L_{md} - L_{mq})(i_{qs}i_{Ds} + i_{Qs}i_{ds})}_{\text{Reluctance Torque}} + \underbrace{2L_{md}i_{df}i_{Qs}}_{\text{Excitation Torque}} + \underbrace{2L_{md}i_{dcg}i_{Qs} - 2L_{mq}i_{qcg}i_{Ds} - (L_{md} - L_{mq})(i_{qcg}i_{Ds} + i_{qcg}i_{ds})}_{\text{Induction Torque}} \right\} \quad (36)$$

From equation (36), it can be seen that the electromagnetic torque of this hybrid machine has three major components. The first component is the reluctance torque. This reluctance torque can be seen to comprise three components which are;

- i. Reluctance torque due to the stator main winding.

$$T_{r1} = \frac{3P}{2} (L_{md} - L_{mq}) i_{Ds} i_{Qs} \quad (37)$$

- ii. Reluctance torque due to the stator control winding

$$T_{r2} = \frac{3P}{2} (L_{md} - L_{mq}) i_{ds} i_{qs} \quad (38)$$

- iii. Reluctance torque due to the interaction between the stator main and control winding

$$T_{r3} = \frac{3P}{2} (L_{md} - L_{mq}) (i_{Ds} i_{qs} + i_{Qs} i_{ds}) \quad (39)$$

The second component is the excitation torque. This torque is as a result of the field excitation. The third component is the induction torque. This component of the torque vanishes once the machine attains the synchronous speed and it is as a result of the interaction between the stator windings and the caged windings.

The rotational motion of the motor is

$$\begin{cases} P\omega_r = (T_e - T_L)/J \\ \theta_r = \int \omega_r dt \end{cases} \quad (40)$$

Where J is the moment of inertia, T_L is the load torque and ω_r is the rotor mechanical speed.

V. THE SIMULATION RESULT

In the analysis of the performance of this machine, we will look at its performance as a motor under which it will be observed under step load and ramp loading.

A. Simulation Result Under Step Load

The dynamic performance analysis of this hybrid synchronous machine is carried out using the parameters of a 4-pole, 5kW, 220V, 50Hz, 3-phase line-start salient-pole synchronous machine. The unsaturated inductances of the machine are: $L_{md}=0.0211H$, $L_{mq}=0.0182H$, $L_{ls}=0.00095H$, $L_{lfr}=0.0009H$, $L_{ldr}=L_{lqr}=0.001375H$, $r_s=1.05\Omega$ and $\eta_{lfr}=21\Omega$.

The effect of saturation was confined to the direct axis and did not affect the quadrature axis and given by the polynomial curve fits. These parameters are expressed as a function of the flux linkages and used to adjust the direct axis inductance and are given as [11], [12]

$$L_d = 0.221e^{(-0.91i_s + 0.21i_s^2 - 0.025i_s^3)} H \quad (41)$$

The magnetic flux due to the field excitation is assumed not to have been affected by the saturation.

The speed of the machine is shown in figure 3.

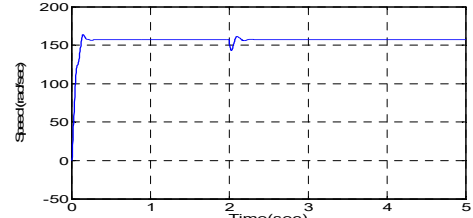


Figure 3: Torque-speed characteristics of the hybrid machine

The reluctance torque component of the machine is shown in figure 4.

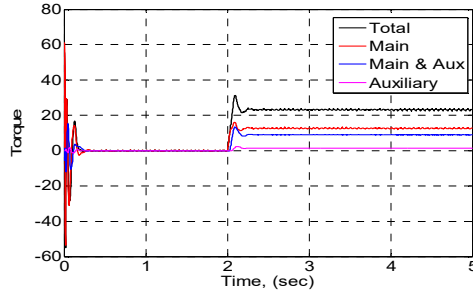


Figure 4: Reluctance torque

Figure 4 show the three components of the reluctance torque and the summation. The comparative view of the excitation and the total reluctance torque is shown in figure 6.

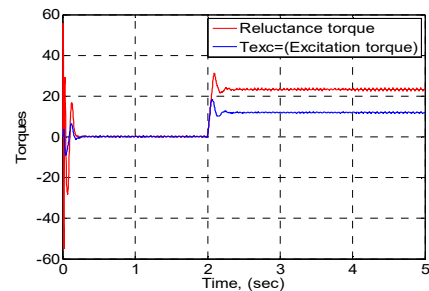


Figure 6: Comparative view of excitation and reluctance torque

B. Simulation Under Ramp Loading

The loading capability of the machine can be observed under ramp loading. The speed and torque characteristics are shown in figures 7 and 8

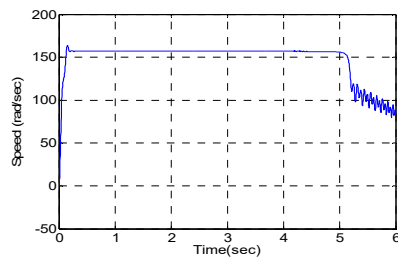


Figure 7: Speed characteristics under ramp loading

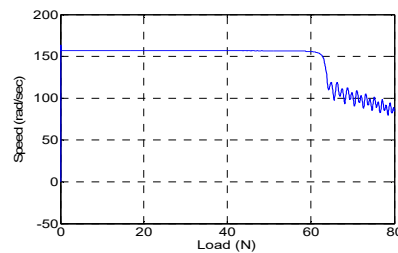


Figure 8: Speed load characteristics under ramp loading

VI. CONCLUSION

A hybrid synchronous machine is modeled and the dynamic performance analysis carried out. The modeled machine has a higher reluctance to excitation torque ratio. This machine has the capability of making the reluctance torque component more than four times the excitation component depending on the value of the capacitor at the auxiliary winding of the machine.

This machine will find application in renewable energy resources when used in micro-hydro power generation and wind energy harvesting due to variability of the reactance ratio.

REFERENCES

- [1] L. U. Anih, E. S. Obe, and S. E. Abonyi, "Modelling and performance of a hybrid synchronous reluctance machine with adjustable X_d / X_q ratio," *IET Electr. Power Appl.*, no. November 2013, pp. 171–182, 2015, doi: 10.1049/iet-epa.2014.0149.
- [2] T. Yuan *et al.*, "Improved synchronous machine rotor design for the easy assembly of excitation coils based on surrogate optimization," *Energies*, vol. 11, no. 5, pp. 1–15, 2018, doi: 10.3390/en11051311.
- [3] C. C. Awah and O. I. Okoro, "The Impact of Machine Geometries on the Average Torque of Dual - Stator Permanent Magnet Machines," *Niger. J. Technol.*, vol. 36, no. 4, pp. 1150–1154, 2017, doi: <http://dx.doi.org/10.4314/njt.v36i4.22>.
- [4] J. Rizk, M. H. Nagrial, and A. Hellany, "Optimum Design Parameters for Synchronous Reluctance Motors," *IME Power Syst. Conf.*, 2004, [Online]. Available: <http://www.techniques-ingenieur.fr/res/pdf/encyclopedia/42249210-d3680.pdf>.
- [5] P. Yulong, S. Yanwen, Y. Yanjun, C. Feng, and L. Yue, "Increasing the saliency ratio of fractional slot concentrated winding interior permanent magnet synchronous motors," *IET Electr. Power Appl.*, vol. 9, no. 7, pp. 439–448, 2015, doi: 10.1049/iet-epa.2014.0336.
- [6] L. U. Anih and E. S. Obe, "Performance analysis of a composite dual-winding reluctance machine," *Energy Convers. Manag.*, vol. 50, no. 12, pp. 3056–3062, 2009, doi: 10.1016/j.enconman.2009.08.008.
- [7] L. U. Anih and E. S. Obe, "Performance analysis of a composite dual-winding reluctance machine," *Energy Convers. Manag.*, vol. 50, pp. 3056–3062, 2009, doi: 10.1016/j.enconman.2009.08.008.
- [8] E. O. Agbachi, L. U. C. A. Anih, and E. S. Obe, "Steady-State Analysis of Hybrid Synchronous Machine With Higher Reluctance to Excitation Power Ratio," *Iran. J. Electr. Electron. Eng.*, vol. 18, no. 1, pp. 1–12, 2022, [Online]. Available: ijeee.iust.ac.ir.
- [9] P. C. Krause, W. Oleg, and S. D. Scott, *Analysis of Electric Machinery and Drive System*, Second. A John Wiley & Sons, Inc. Publication, 2002.
- [10] Chee-Mun Ong, *Dynamic Simulation of Electric Machinery using Matlab/Simulink*. New Jersey: Printice Hall PTR, 1998.
- [11] O. Ojo and J. Cox, "Investigation into the performance characteristics," in *Industry Applications Conference*, 1996, pp. 533–540.
- [12] G. Todorov and B. Stoev, "Saturation effects on the parameters of interior permanent magnet synchronous motors with different rotor configuration," *Mater. Sci. Forum*, vol. 856, pp. 257–262, 2016, doi: 10.4028/www.scientific.net/MSF.856.257.